This is the author submitted manuscript of

«An open-loop control scheme to increase the speed and reduce the viscoelastic drift of dielectric elastomer actuators»

By A. Poulin and S. Rosset
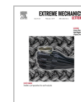
Published in Extreme Mechanics Letters, 2019

doi: 10.1016/j.eml.2019.01.001

https://doi.org/10.1016/j.eml.2019.01.001

An open-loop control scheme to increase the speed and reduce the viscoelastic drift of dielectric elastomer actuators

Alexandre Poulin [a] ✉ , Samuel Rosset [b] ✉

Show more ∨

+ Add to Mendeley   ⁂ Share   ❞ Cite

Get rights and content ↗

An open-loop control scheme to increase the speed and reduce the viscoelastic drift of dielectric elastomer actuators

Alexandre Poulin[a], Samuel Rosset[b,*]

[a]*École polytechnique fédérale de Lausanne (EPFL), Soft Transducers Laboratory, Neuchâtel, Switzerland*
[b]*University of Auckland, Auckland Bioengineering Institute, Biomimetics Lab, Auckland, New Zealand*

Abstract

We present a simple open-loop method to increase the response speed and suppress the viscoelastic creep of dielectric elastomer actuators. The parameters of the model can be extracted from two simple measurements: a strain vs. voltage ramp, and the strain response to a voltage step. We demonstrate the method by generating different strain profiles on actuators made with VHB or silicone membranes. We show an efficient reduction of the viscoelastic drift, and an increase in response speed by a factor of 150 for VHB actuators, and 25 for silicone actuators.

Keywords: dielectric elastomer actuators, soft actuators, open-loop control, viscoelasticity

1. Introduction

Dielectric elastomer actuators (DEAs) are soft actuators that generate large actuation strains [1]. This makes them interesting for various fields of application including soft robotics, tuneable optics, microfluidics, mechanical loading of cells, and haptic interfaces [2, 3]. The structure of a DEA consists of a soft elastomeric dielectric membrane sandwiched between two compliant electrodes, thus forming a rubbery capacitor that deforms upon application of a voltage [4]. When an electric field is applied between the electrodes, the generated Maxwell pressure causes a squeezing of the dielectric membrane, which decreases in thickness and increases in surface.

Two different classes of elastomers are predominantly used to manufacture DEAs: silicones, and acrylic elastomers (mainly the commercial adhesive tape *VHB* from 3M) [5, 6]. Both of these materials are viscoelastic and therefore

---

*Corresponding author
Email addresses: `alexandre.poulin@epfl.ch` (Alexandre Poulin), `s.rosset@auckland.ac.nz` (Samuel Rosset)

present a time-dependent strain response to a stress input, thus making the precise control of a DEA difficult. This is particularly true of VHB which has a very low mechanical bandwidth with mechanical relaxation times of several hundreds of seconds [7]. Closed loop control of DEA driven systems enables to compensate the viscoelastic drift but requires external sensors, which is not always practical. Alternatively, the actuator itself – being a soft capacitor – can be used as a sensor. This self-sensing approach has been pioneered by Gisby et al. and used to drive DEAs in close-loop mode [8]. Although this method doesn't require external sensors to measure the strain, it still needs a specific power supply that provides the high voltage to drive the actuators and the self-sensing capabilities [9]. From our experience, this approach doesn't work well on VHB actuators [10].

In this contribution, we present a simple open-loop method to account for the viscoelastic response of DEAs, and to calculate the voltage signal required to obtain a desired strain output. The viscoelastic behaviour of the elastomer materials used to manufacture DEAs has been investigated in detail in the literature. Most of the studies are based on a quasi-linear viscoelastic model, such as Kelvin-Voigt, or Kelvin-Voigt-Maxwell, combining a non-linear stress-strain relationship with a strain-independent relaxation curve [7, 11–15]. Although the viscoealstic creep of DEAs has been extensively modeled, there are fewer reports on how these models can be used to compensate the viscoelastic drift of DEAs. Zhang et al. have presented a model to stabilise the strain of a DEA after it has reached a target value. They demonstrate a dot actuator driven with $2.5\,\mathrm{kV}$, which reaches $12.5\,\%$ actuation strain after $200\,\mathrm{s}$. Once this target strain is reached, their model enables to calculate the voltage profile required to stabilise the strain at this value [16]. Zou et al. presented a phenomenological model to compensate the transient vibrations of a DEA driving an inertial mass, as well as to suppress the viscoelastic creep, in the case of a strain step [17]. For the creep suppression, they define an arbitrary time of $7\,\mathrm{s}$ at which creep starts, and the strain of the actuator at that moment is defined as the ideal strain that must be maintained. They have further developed their control method to sinusoidal strain output, using the hysteresis loop to compensate for viscoelasticity, in combination with a conventional closed-loop PI controller [18].

Our approach is based on a quasi-linear viscoelastic model of the elastomer, which is represented as a generalised Kelvin-Voigt model with different time constants. It enables calculating the voltage profile to reach an arbitrary strain value from the start of the step, without the need to wait until a target strain is reached. This enables to hit the target strain quickly, and to increase the response speed of DEAs by a factor up to 150 for VHB-based actuators. Our model-based approach relies on two simple tests to characterise the system, and enables to calculate the required voltage input not only for a step strain response, but for any desired output profile. We separate the response of the actuator into the steady-state response, and the dynamic viscoelastic response. We neglect inertia, which is valid for an actuator acting on a negligible mass, such as our device designed to stretch biological cells [19, 20], a tunable grating [10, 21, 22], etc. However, our model can be further expanded to account for

the effect of inertia.

2. Viscoelastic model

The steady state response of the actuator represents the actuator state once equilibrium has been reached. We represent it with a function f, which links the output steady-state strain ε_{ss} to the applied voltage V:

$$\varepsilon_{ss} = f(V) \tag{1}$$

In the most simple case of linear elasticity, and for a case of free boundary conditions, the relation between the in-plane axial strain and the voltage is given by the following equation, if we assume that the thickness of the actuator remains constant [4]:

$$f(V) = \varepsilon_x = \varepsilon_y = -\frac{\varepsilon_z}{2} = \frac{\epsilon V^2}{2Y z_0^2}, \tag{2}$$

with $\varepsilon_{x,y}$ the in-plane strain, ε_z the thickness strain, ϵ the permittivity of the dielectric, Y the Young's modulus of the material, and z_0 the initial thickness of the membrane. The Maxwell stress causes a thickness reduction of the membrane (ε_z), but this effect is usually more difficult to measure than the in-plane expansion of the electrode. For the small deformation approximation used here, the in-plane deformation is linked to the thickness strain by the Poisson ratio, taken to be 0.5 for incompressible materials: $\varepsilon_x = \varepsilon_y = -\varepsilon_z/2$. In this work, we will measure the in-plane expansion of the electrode with a camera, and we therefore define the in-plane strain as the steady-state strain in eq. 2. Reference [4] also presents a modified form of eq. 2 that accounts for the fact that the actuator thickness reduces with the applied voltage. Usually, planar DEAs use prestretch to absorb the expansion of the active zone into the passive zone, and to enhance the electromachanical properties and breakdown strength of the membrane. Therefore, even if the actuation strain remains in the 0 % to 20 % range, eq. 2 is often not adequate to model the actuation strain, because the prestretch of the membrane causes it to operate in a non-linear region of the stress-strain curve. Consequently, hyper-elastic models based on a strain energy density function are often used to describe the static (i.e. steady-state) relationship between stretch of the membrane and the applied voltage [23–25]. Different hyperelastic strain energy density functions have been used to model DEAs, such as Neo-Hookean [23], Gent [25], Yeoh, or Ogden [7]. In the case of hyperelastic models, it is often easier to express the voltage as a function of strain, i.e. $V = f^{-1}(\varepsilon_{ss})$. For the particular case of an in plane actuator (such as the ubiquitous expending circle actuator [1, 26]) modelled using a Neo-Hookean strain energy density function, the driving voltage as a function of strain is given by:

$$V = f^{-1}(\varepsilon_{ss}) = \sqrt{\frac{\mu t_0^2}{\epsilon \lambda_a^3 \lambda_p^3} \left(\lambda_a \lambda_p - (\lambda_a \lambda_p)^{-5} - \lambda_p + \lambda_p^{-5} \right)}, \tag{3}$$

where μ is the shear modulus of the elastomer, t_0 the initial thickness (before prestretch) of the membrane, λ_a the actuation stretch, linked to the actuation strain by the relation $\lambda_a = (\varepsilon_{ss} + 1)$, and λ_p the equi-biaxial prestretch in the membrane. The derivation of this relation, which assumes an active area much smaller than the overall membrane diameter, is given in the supplementary information. The unknown parameters of $f(V)$ can be obtained using curve fitting on a strain versus voltage ramp performed slowly to be in steady state mode. Simpler numerical approximations or empirical models can be used. For the tunable grating presented in section 4, we have used quadratic Lagrangian interpolation between measured experimental points to remove the need of an analytical model. For our cell-stretching device, whose output strain typically lies in the $0\,\%$ to $30\,\%$ range, we have obtain good fitting (c.f. section 4) with the following empirical equation:

$$f(V) = KV^n, \tag{4}$$

where K and n are two constants obtained by fitting. This empirical model is similar to eq. 2, with K combining the influence of the permittivity, the Young's modulus, and the thickness of the membrane. The parameter n is experimentally found to be around around 3, thus leading to a strain that increases more quickly with voltage compared to the quadratic relation of eq. 2. This is not surprising, as the basic model does not account for the membrane thickness reduction caused by the in-plane actuation. The parameters K and n depend on the amount of prestrain applied to the membrane. Comparing membranes of equal thickness after prestrain, the value of K decreases with prestrain, due to the increase of stiffness of the material at larger strains. We have also observed that the parameter n tends to decrease with increasing prestretch, which can be explained by the actuation-stretch-induced stiffening of the material partly compensating the reduction in membrane thickness. Highly pre-stretched membranes tend to deviate from the empirical model, and other methods (hyperelastic model or data interpolation) should be used in case the the above model doesn't provide an adequate prediction of the steady-state behaviour of the actuator.

If the voltage applied to the actuator is not a constant, but a time dependent function (i.e. $V = V(t)$), then the function f cannot be used to describe the output strain $\varepsilon(t)$ of the actuator, unless the rate of change of the voltage is very slow compared to the relaxation time of the viscoelastic processes. More generally, the output time-dependent strain $\varepsilon(t)$ is defined in the Laplace domain by the equation:

$$E(s) = F(s)H(s), \tag{5}$$

where $E(s)$, and $F(s)$ are the Laplace transform of $\varepsilon(t)$ and $f(V(t))$, and $H(s)$ is the transfer function (impulse response) of the actuator.

Therefore, given a target strain output profile $\varepsilon(t)$ of the actuator, the required input voltage can be calculated by combining Eq. 1 and Eq. 5:

$$V(t) = f^{-1}\left(\mathscr{L}^{-1}\frac{E(s)}{H(s)}\right). \tag{6}$$
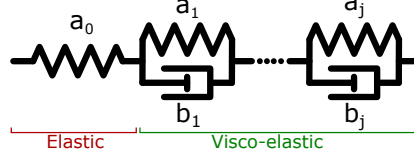
Figure 1: Model of the elastomer as an elastic element and a series of Kelvin-Voigt elements that characterise the different time constants of the material. The a_i coefficients represent the relative amplitude of each element. The b_i coefficients represent the inverse of the time constant of each element.

When using the empirical voltage-strain relation introduced above (Eq. 4), we obtain:

$$V(t) = \sqrt[n]{\frac{1}{K} \mathscr{L}^{-1}\left(\frac{E(s)}{H(s)}\right)}. \tag{7}$$

To define the impulse response $H(s)$, the viscoelastic response of the actuator is modelled by representing the actuator as a spring (purely elastic response) in series with a variable number of Kelvin-Voigt elements (spring in parallel with a damper) representing the different relaxation times of the elastomer (Fig. 1) [12]. This leads to the following time-dependent strain response $\varepsilon(t)$ to a step stress input:

$$\varepsilon(t) = \varepsilon_{ss} \left(a_0 + \sum_{i=1}^{j} a_i \left(1 - e^{(-b_i t)} \right) \right), \tag{8}$$

where the coefficients $1/b_i$ are the different time constants of the viscoelastic relaxation processes, each having a strain weighting factor a_i, with a_0 representing the weight of the elastic (i.e. instantaneous) response. The sum of all a_i coefficients, from $i = 0$ to j, must be 1. ε_{ss} is the steady-state response of the actuator (Eq. 1), and it can be verified that $\varepsilon(t)$ approaches ε_{ss} when t approaches infinity. The model parameters a_i and b_i can be obtained using a non-linear curve fit on the strain versus time data resulting from a voltage step.

We take the Laplace transform of Eq. 8 and note that it is the step response of the system. Therefore, the transfer function (impulse response) $H(s)$ is given by:

$$\mathscr{L}\left(\varepsilon(t)\right) = \varepsilon_{ss} \left(\frac{a_0}{s} + \sum_{i=1}^{j} \frac{a_i b_i}{b_i s + s^2} \right) = \frac{\varepsilon_{ss}}{s} H(s) \tag{9}$$

$$H(s) = a_0 + \sum_{i=1}^{j} \frac{a_i b_i}{b_i + s}. \tag{10}$$

3. Step strain response

We first consider the special case of a step strain response: what voltage function should be applied to obtain a strain step output of amplitude ε_{ss}

5

$(E(s) = \varepsilon_{ss}/s)$? We consider the case of an elastomer which can be modelled with two time constants (i.e. $j = 2$ in Eq. 10). As shown in the experimental section (c.f. section 4), this is adequate for VHB and silicone actuators measured with a 3 Hz sampling rate over 600 s. We calculate $E(s)/H(s)$ for this particular case:

$$\frac{E(s)}{H(s)} = \frac{\varepsilon_{ss}}{s} \frac{s^2 + s(b_1 + b_2) + b_1 b_2}{s^2 a_0 + s(a_0(b_1 + b_2) + a_1 b_1 + a_2 b_2) + b_1 b_2}, \tag{11}$$

and introduce the coefficients N_i and D_i for the numerator and denominator of the transfer function, which depend on parameters a_i and b_i:

$$\frac{E(s)}{H(s)} = \varepsilon_{ss} \frac{s^2 + N_1 s + N_0}{D_3 s^3 + D_2 s^2 + D_1 s}. \tag{12}$$

To go back in the time domain, we calculate the inverse Laplace transform using a mathematical computing engine:

$$\mathscr{L}^{-1}\left(\frac{E(s)}{H(s)}\right) = \varepsilon_{ss}\left(1 + Ae^{\alpha t} + Be^{\beta t}\right), \tag{13}$$

with

$$A = \frac{U - V - W + X + Y}{Z}$$
$$B = \frac{-U - V + W - X + Y}{Z}$$
$$T = \sqrt{D_2^2 - 4D_1 D_3}$$
$$U = D_2 D_3 N_0 \qquad V = D_3 N_0 T$$
$$W = 2D_1 D_3 B_1 \qquad X = D_1 D_2$$
$$Y = D_1 T \qquad Z = 2D_1 D_3 T$$
$$\alpha = \frac{-T - D_2}{2D_3} \qquad \beta = \frac{T - D_2}{2D_3}. \tag{14}$$

Finally, by combining Eq. 13 and Eq. 7, we can give an analytical voltage function that leads to a step strain output of amplitude ε_{ss} :

$$V(t) = \sqrt[n]{\frac{\varepsilon_{ss}}{K}\left(1 + Ae^{\alpha t} + Be^{\beta t}\right)}. \tag{15}$$

For cases that require more than 2 time constants to model the material, or for a target strain profile $\varepsilon(t)$ other than a step function, Eq. 6 can be solved numerically to compute $V(t)$. Numerical solving also allows to replace the empirical approximation for $f(V)$ by an hyperelastic constitutive model such as the neo-hookean example of Eq. 3, or a numerical method such as Lagrangian interpolation.
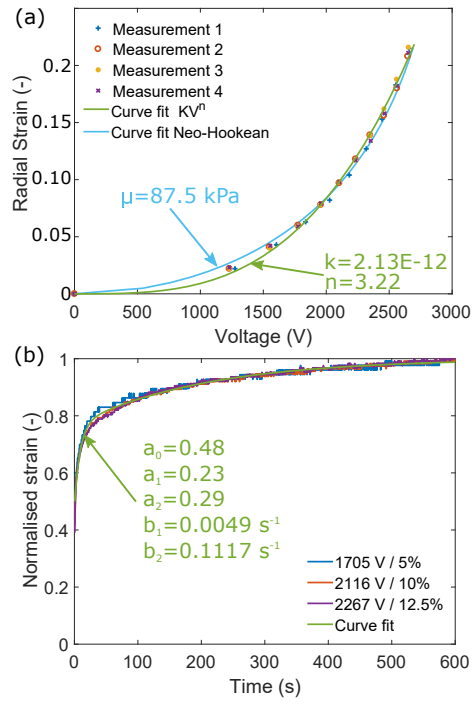
Figure 2: a)Steady-state radial strain versus voltage on a VHB actuator, and fit with a Neo-Hookean model (Eq. 3) and the empirical model (Eq. 4). b) Normalised strain versus time for a step input voltage of three different amplitudes, and fit with Eq. 8.

4. Experimental Validation

To test the validity of our approach, we have fabricated expending-circle actuators [1, 26] with silicone and VHB membranes. The actuators consist of a membrane equi-biaxially prestretched and fixed on a 44 mm diameter circular frame, with a 4 mm diameter electrode patterned at the centre of each side of the membrane. An automated measurement set-up using a camera and a LabVIEW program measures the diameter of the actuators as a function of applied voltage. We use cross-correlation to measure the actuator diameter with a sub-pixel resolution. The camera is set-up so that the initial diameter of the actuator is at least 1000 pixels, thus providing a strain resolution better than 0.1 %.

The VHB actuators are made by prestretching a 500 μm film of VHB4905 by a factor 3 in both directions, leading to a final calculated thickness of 56 μm. The electrodes are made of carbon grease (Nyogel 756) manually smeared through a stencil. First, a measurement ramp is performed to characterise the strain as a function of the applied voltage in the 0 % to 20 % strain range (Fig. 2 a). A waiting time of 120 s is applied to each measurement point to ensure steady-state, and the measurement is repeated 4 times. Both the Neo-Hookean (Eq. 3) and the empirical voltage-strain relationship (Eq. 4) are fitted to the data. For the Neo-Hookean model, the initial thickness of the membrane t_0 is 500 μm, the prestretch λ_p is 3, and the permittivity of the dielectric is taken to be $4.11 \times 10^{-11} \, \mathrm{F\,m^{-1}}$ [27]. The fit leads to a shear modulus μ of 87.5 kPa, which is close to the 65 kPa to 85 kPa range published in the literature [25, 27]. Direct comparison can however not be made, as these values have been obtained in different conditions.

The fit of the data with the empirical model leads to $K = 2.13E-12$ and $n = 3.22$ and represents a very good fit in the tested strain range We therefore use it here, as it leads to a much simpler analytical formulation. This steady-state strain-voltage relation is then used to calculate the voltage required to reach a strain of 5 %, 10 %, and 12.5 % (1705 V, 2116 V, and 2267 V). Voltage steps of these amplitudes are performed and held for 600 s, during which the strain versus time is recorded, and normalised (Fig. 2 b). The time-dependent strain response (Eq. 8) is fitted to the data to extract the values of the parameters a_i and b_i. In accordance with the special case of Eqs. 12 to 14, we use 2 time constants, leading to a good approximation of the experimental data (Fig. 2 b). The two time constants resulting from the fit are 202 s with a contribution of 23 % of the total response, and 8.95 s with a contribution of 29 %. The purely elastic (i.e. instantaneous) response has a contribution of 48 %. The camera used to measure the strain has a frame rate of 3 fps, and any viscoelastic process with a time scale lower than 1/3 s appears as instantaneous. The parameters a_i and b_i are then used with Eqs. 12 to 14 to calculate the values of A, B, α, and β. The numerical values of the model parameters obtained for this actuator are summarised in table 1.

We have then used the model parameters to calculate the voltage profile required to produce step strain responses (Eq. 15) with amplitudes of 4 %,

8

$K = 2.13e - 12$	$n = 3.21$
$a_0 = 0.48$	
$a_1 = 0.23$	$b_1 = 0.0049 \text{ s}^{-1}$
$a_2 = 0.29$	$b_2 = 0.1117 \text{ s}^{-1}$
$A = 0.79$	$\alpha = -0.1790 \text{ s}^{-1}$
$B = 0.29$	$\beta = -0.0064 \text{ s}^{-1}$

Table 1: Model parameters for the VHB actuator with grease electrodes. The first line shows the parameters of the empirical steady-state strain-voltage model. The next 3 lines give the parameters of the transfer function that can be used to calculate arbitrary outptut strain profiles. The last 2 lines give the parameters for the special case of a step strain output (Eq. 15).
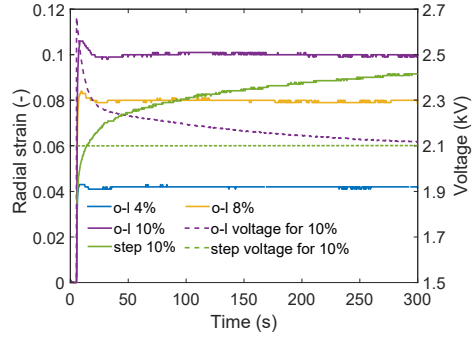

Figure 3: Application of the open-loop (o-l) model to generate a step strain response with different amplitude for the VHB actuator. For the 10 % strain step, we have also included the voltage profile applied to the actuator. The response to a step voltage to reach 10 % strain is given for comparison. The response time of the open-loop model is 150 times faster than for a voltage step.
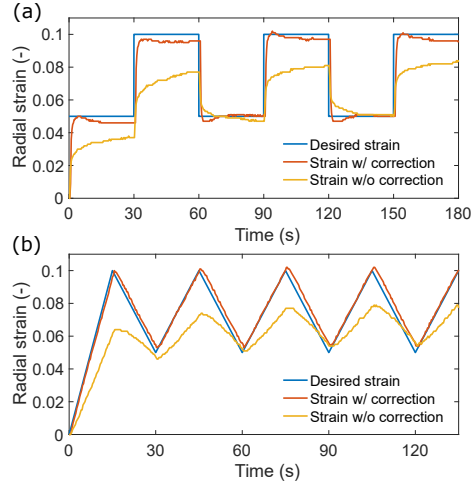
Figure 4: Waveforms from 5 % to 10 % strain for the VHB actuator with and without open-loop correction. a) square waveform. b) triangle waveform.

8 %, and 10 % (Fig. 3). The responses show a small overshoot, followed by a constant strain plateau of the desired amplitude. As a comparison, the strain profile obtained by using a simple step voltage input to reach 10 % strain is also shown on the figure. Using the corrected voltage profile, it takes 1.5 s for the signal to settle within ± 10 % of the final value and 245 s when using a simple voltage step. Our method therefore increases by more than 150 times the response speed of VHB actuators. Because of the slight overshoot (to 10.6 % in case of the 10 % strain step), the response speed gain is reduced to 52, if the tolerance band for the settling time is decreased to ±5 %

To demonstrate the versatility of the method, we have calculated voltage functions leading to different strain output profiles for the same actuator (using the parameters of the first 4 lines of Table 1). We apply Eq. 7 numerically to calculate the required voltage input given a target output strain profile. Fig. 4 a shows the output strain obtained for a targeted square signal between 5 % and 10 % with a period of 60 s. The voltage computed using the viscoelastic model leads to an output strain that is very close to the desired output, whereas the strain obtained without the viscoelastic correction (that is by calculating the voltage profile using Eq. 4) exhibits a smaller amplitude and a drift during the holding time. Similar results are obtained for other waveforms, such as a triangle (Fig. 4 b).

The parameters of the model are influenced by the membrane material, its prestretch, and the type of electrode used to make the actuator. Therefore, a group of actuators produced using the same parameters share the same required voltage input to reach a targeted strain. It is thus only necessary to characterise one actuator to identify the parameters of the model, which can then be applied to the whole group of similar actuators. To demonstrate this, we have produced
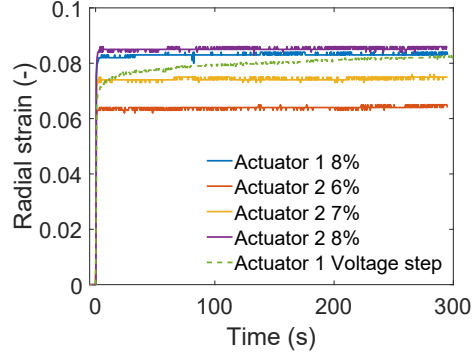
10

Figure 5: Strain step response of different amplitudes on 2 different silicone actuators using the same model parameters fitted on data from actuator 1. Response to a step voltage on actuator 1 shown for comparison.
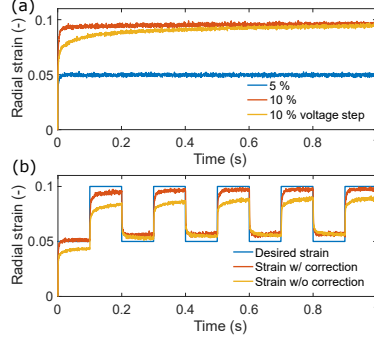

Figure 6: Response of a silicone actuator on a 1 s time frame. a) step strain response. b) strain response for a targeted square strain signal at 5 Hz.

two actuators made with a Dow Corning Sylgard 186 silicone membrane and pad-printed electrodes [29], with the same geometry as the VHB actuator. A voltage ramp and voltage step are performed on actuator 1 to fit the parameters of the model, which are then used to generate voltage profiles for strain step responses of different amplitudes. The results show that the model parameters of actuator 1 can be successfully applied on actuator 2 (Fig. 5). Actuator 2 has a slightly thinner membrane (36 µm versus 37 µm for actuator 1), which can explain the higher strain values reached by actuator 2.

One of the advantages of actuators made with a silicone membrane is that they have a much higher response speed than VHB actuators [14, 30]. We have therefore characterised the strain response of silicone actuators on a 1 s time-scale, using a high speed camera to capture the radial strain at 2800 frames/s. To account for the faster response speed while keeping the ability to model the slower viscoelastic drift, the voltage step response was modelled with 3 different time constants (parameters b_i of $1/1.25\,\mathrm{ms}^{-1}$, $1/45\,\mathrm{ms}^{-1}$, and $1/475\,\mathrm{ms}^{-1}$). We
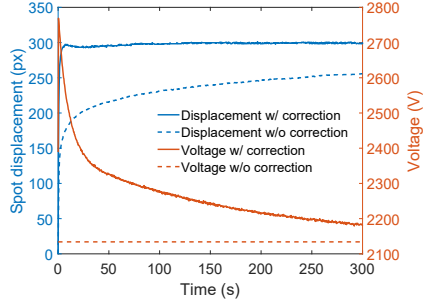
11

Figure 7: Displacement of the first order diffraction spot of a DEA tuneable grating on a screen for a targeted displacement of 300 pixels. The continuous curves show the displacement and voltage using the model, and the dashed curve show the displacement and voltage obtained with a constant voltage.

apply the model to calculate the voltage waveforms required to obtain strain steps of 5 % and 10 % (Fig. 6 a). The response of the actuator to a voltage step leading to final strain of 10 % is also given for comparison. The model enables to reach the targeted strain very quickly and to hold it to the desired value. For the 10 % case, the actuator needs 8.5 ms to settle within ± 10 % of the final strain value, whereas it needs 230 ms when a voltage step is used, which represents an increase by a factor of 27. The model is used to obtain a square strain response from 5 % to 10 % at 5 Hz. Using the model to compute the voltage leads to an output strain which is much closer to the desired amplitude and that remains constant during the holding time (Fig. 6 b).

Finally, we apply the method to control a soft optical tuneable grating. Tuneable optical devices are an interesting application for DEAs, thanks to the large tuning range they provide[21, 22, 30]. However, most optical applications require the possibility to hold a given position over time, without viscoelastic drift [3]. In a previous contribution, we used capacitive self-sensing to implement a close-loop control of a soft optical tunable grating based on DEAs [10]. We showed that even though we could regulate the voltage to keep the capacitance of the device to a constant value, the grating period, and therefore the diffraction angle, was drifting over time for VHB actuators. Although the cause of this drift was not identified, it is speculated that either some stress relaxation or dipole reorientation causes the dielectric permittivity to change over time. Here, instead of closed-loop operation based on capacitive self-sensing, we apply our open-loop method to control the diffraction angle of a tuneable grating. A device similar to that presented in [10] is fabricated. Briefly, a VHB film of 500 μm initial thickness is prestretched equi-biaxially by a factor of 3 and fixed on a square frame with a 60 mm opening. A 10 mm soft grating with 500 lines/mm is placed at the centre of the membrane, and electrodes are applied on both sides of the grating, so that their expansion compresses the soft grating. A picture of the device is included in the supplementary information (figure S1). The device is mounted parallel to a paper screen with a separation of 60 mm.

12

A red laser (650 nm) is shone through the grating, and the displacement of the first order diffraction point is measured with a camera. We record the on-screen displacement (in pixel) of the first order diffraction spot. We first measure the steady-state displacement of the spot between 0 V to 3000 V, followed a step voltage input to 3000 V held for 10 min. After identification of the model parameters, we calculate the voltage profile required to move the laser spot by 300 pixels. In this case, we use quadratic Lagrangian interpolation between the experimental data points to model the steady state behaviour, and a viscoelastic relaxation (Eq. 8) with two time constants. The data and fit are shown in the supplementary information (Figure S1). As a comparison, we also measure the position of the spot for a voltage step of 2130 V, which is the voltage leading to a steady state displacement of 300 pixels. Figure 7 shows the spot displacement and voltage profile for the two cases. When using the model to calculate the voltage input profile, it takes 1.7 s for the spot to settle within ±10 % of its total displacement. It then remains very stable at the targeted displacement of 300 pixels and shows a clear improvement compared to the step voltage input. After 30 s, the displacement of the spot is constrained between 293 and 301 pixels. In the case of the voltage step input, it takes 226 s for the signal to settle within ±10 % of its total displacement. The open-loop model increases the response speed by a factor of 133, which is similar to the value of 150 obtained for the circular DEA actuator. If the error band used to identify the settling time is reduced to ±5 %, the open-loop method provides a speed gain of 128. This is better than for the circular VHB actuator, due to the absence of the overshoot for the grating actuator.

5. Conclusions

In summary, we presented a simple model to calculate the voltage input of a DEA that leads to a target strain output. Although this approach cannot compensate for external perturbations as a closed-loop approach would, it doesn't require external sensors, and it is well adapted for applications in which the actuator doesn't need to act against varying external forces, such as the mechanical stretching of biological cells [19, 20], or tuneable optical diffraction gratings [10]. For the cell-stretching application, we have previously used voltage functions found by trial and error to increase the response speed of our silicone-based actuators [20]. The current approach defines a simple method to calculate the desired voltage profile, based on basic characterisation of the actuator (voltage ramp and step response). Compared to the trial-and-error waveform presented in [20], the model presented here does not create a strain overshoot and leads to a better strain stabilisation. For the tuneable grating, we have shown how our approach can be used to control the diffraction angle of a tuneable grating based on a VHB dielectric elastomer actuator. With the open-loop method to control the grating compression, we have obtained a settling time of 1.7 s and a better stability compared to our capacitive self-sensing approach presented in [10]. The method has been tested on actuators

made with VHB and silicone and has shown its ability to suppress the viscoelastic drift, increase the response speed, and generate arbitrary strain waveforms. The method is based on the assumption that the dynamic response of the actuator is not dependent on the strain magnitude, i.e. that the coefficients a_i and b_i from Eq. 8 are independent from the value of ε_{ss}. This makes the time and strain contributions separable and therefore only requires two separate tests to identify the parameters of the model. We have observed that silicone actuators under equi-biaxial prestretch up to 1.4, or anistoropically prestretched by a factor 1.2×2.7 (configuration of the cell stretcher [20]) exhibit this behaviour over their full voltage range, and are therefore good candidates for this method. VHB actuators tend to deviate from this assumption for strains above 20 % (c.f. Figure S2 in the supplementary information), and a more complex model based on non-linear viscoelasticity should be used to accurately control VHB at large strains. Most real-world applications of DEAs are based on silicone membranes with actuation strains in the 5 % to 20 % range, for which the model presented here can be advantageously used to control the strain output profile.

6. Acknowledgements

References

[1] R. Pelrine, R. Kornbluh, Q. Pei, and J. Joseph. High-speed electrically actuated elastomers with strain greater than 100%. *Science*, 287(5454):836–839, 2000.

[2] Iain A. Anderson, Todd A. Gisby, Thomas G. McKay, Benjamin M. O'Brien, and Emilio P. Calius. Multi-functional dielectric elastomer artificial muscles for soft and smart machines. *Journal of Applied Physics*, 112(4):041101, 2012.

[3] Samuel Rosset and Herbert R. Shea. Small, fast, and tough: Shrinking down integrated elastomer transducers. *Applied Physics Reviews*, 3(3):031105, 2016.

[4] R. E. Pelrine, R. D. Kornbluh, and J. P. Joseph. Electrostriction of polymer dielectrics with compliant electrodes as a means of actuation. *Sensors and Actuators, A: Physical*, 64(1):77–85, 1998.

[5] Frederikke B. Madsen, Anders E. Daugaard, Søren Hvilsted, and Anne L. Skov. The current state of silicone-based dielectric elastomer transducers. *Macromol. Rapid Commun.*, 37(5):378–413, 2016.

[6] P. Brochu and Q. Pei. Advances in dielectric elastomers for actuators and artificial muscles. *Macromolecular Rapid Communications*, 31(1):10–36, 2010.

[7] M. Wissler and E. Mazza. Mechanical behavior of an acrylic elastomer used in dielectric elastomer actuators. *Sensors and Actuators, A: Physical*, 134(2):494–504, 2007.

[8] Todd A. Gisby, Benjamin M. O'Brien, Sheng Q. Xie, Emilio P. Calius, and Iain A. Anderson. Closed loop control of dielectric elastomer actuators. In *Proceedings of SPIE - The International Society for Optical Engineering*, volume 7976, pages 797620–797620–9, 2011.

[9] Todd A. Gisby, Benjamin M. O'Brien, and Iain A. Anderson. Self sensing feedback for dielectric elastomer actuators. *Applied Physics Letters*, 102:193703, 2013.

[10] Samuel Rosset, Benjamin M O'Brien, Todd Gisby, Daniel Xu, Herbert R Shea, and Iain A Anderson. Self-sensing dielectric elastomer actuators in closed-loop operation. *Smart Materials and Structures*, 22(10):104018, 2013.

[11] Junshi Zhang, Jie Ru, Hualing Chen, Dichen Li, and Jian Lu. Viscoelastic creep and relaxation of dielectric elastomers characterized by a kelvin-voigt-maxwell model. *Applied Physics Letters*, 110(4):044104, jan 2017.

[12] Michael Wissler and Edoardo Mazza. Modeling and simulation of dielectric elastomer actuators. *Smart Materials and Structures*, 14(6):1396, 2005.

[13] Matthias Kollosche, Guggi Kofod, Zhigang Suo, and Jian Zhu. Temporal evolution and instability in a viscoelastic dielectric elastomer. *Journal of the Mechanics and Physics of Solids*, 76:47–64, 2015.

[14] S. Michel, X.Q. Zhang, C. Wissler, M.and Loewe, and G. Kovacs. A comparison between silicone and acrylic elastomers as dielectric materials in electroactive polymer actuators. *Polymer International*, 59(3):391–399, 2010.

[15] E-F M Henke, Katherine E Wilson, and I A Anderson. Modeling of dielectric elastomer oscillators for soft biomimetic applications. *Bioinspiration & Biomimetics*, 13(4):046009, 2018.

[16] Junshi Zhang, Yanjie Wang, David McCoul, Qibing Pei, and Hualing Chen. Viscoelastic creep elimination in dielectric elastomer actuation by preprogrammed voltage. *Applied Physics Letters*, 105(21):212904, 2014.

[17] Jiang Zou, Guo-Ying Gu, and Li-Min Zhu. Open-loop control of creep and vibration in dielectric elastomer actuators with phenomenological models. *IEEE/ASME Transactions on Mechatronics*, 22(1):51–58, 2017.

[18] Jiang Zou and Guoying Gu. High-precision tracking control of a soft dielectric elastomer actuator with inverse viscoelastic hysteresis compensation. *IEEE/ASME Transactions on Mechatronics*, pages 1–1, 2018.

[19] Alexandre Poulin, Cansaran Saygili Demir, Samuel Rosset, Tatjana Petrova, and Herbert R Shea. Dielectric elastomer actuator for mechanical loading of 2D cell cultures. *Lab on a Chip*, 16(19):3788–3794, 2016.

[20] Alexandre Poulin, Matthias Imboden, Francesca Sorba, Serge Grazioli, Cristina Martin-Olmos, Samuel Rosset, and Herbert Shea. An ultra-fast mechanically active cell culture substrate. *Scientific Reports*, 8(1), 2018.

[21] Yin Wang, Jinxiong Zhou, Wenjie Sun, Xiaohong Wu, and Ling Zhang. Mechanics of dielectric elastomer-activated deformable transmission grating. *Smart Materials and Structures*, 23(9):095010, jul 2014.

[22] Matthias Kollosche, Sebastian Doering, Joachim Stumpe, and Guggi Kofod. Voltage-controlled compression for period tuning of optical surface relief gratings. *Optics Letters*, 36(8):1389–1391, Apr 2011.

[23] Z. Suo. Theory of dielectric elastomers. *Acta Mechanica Solida Sinica*, 23(6):549–578, 2010.

[24] S.J.A. Koh, T. Li, J. Zhou, X. Zhao, W. Hong, J. Zhu, and Z. Suo. Mechanisms of large actuation strain in dielectric elastomers. *Journal of Polymer Science, Part B: Polymer Physics*, 49(7):504–515, 2011.

[25] T. Lu, J. Huang, C. Jordi, G. Kovacs, R. Huang, D.R. Clarke, and Z. Suo. Dielectric elastomer actuators under equal-biaxial forces, uniaxial forces, and uniaxial constraint of stiff fibers. *Soft Matter*, 8(22):6167–6173, 2012.

[26] Federico Carpi, Iain Anderson, Siegfried Bauer, Gabriele Frediani, Giuseppe Gallone, Massimiliano Gei, Christian Graaf, Claire Jean-Mistral, William Kaal, Guggi Kofod, Matthias Kollosche, Roy Kornbluh, Benny Lassen, Marc Matysek, Silvain Michel, Stephan Nowak, Benjamin O'Brien, Qibing Pei, Ron Pelrine, Björn Rechenbach, Samuel Rosset, and Herbert Shea. Standards for dielectric elastomer transducers. *Smart Materials and Structures*, 24(10):105025, 2015.

[27] Michael Bozlar, Christian Punckt, Sibel Korkut, Jian Zhu, Choon Chiang Foo, Zhigang Suo, and Ilhan A. Aksay. Dielectric elastomer actuators with elastomeric electrodes. *Applied Physics Letters*, 101(9):091907, 2012.

[28] Samuel Rosset, Luc Maffli, Simon Houis, and Herbert Shea. An instrument to obtain the correct biaxial hyperelastic parameters of silicones for accurate DEA modelling. In *Proceedings of SPIE - The International Society for Optical Engineering*, volume 9056, page 90560M, 2014.

[29] Samuel Rosset, Oluwaseun A. Araromi, Samuel Schlatter, and Herbert R. Shea. Fabrication process of silicone-based dielectric elastomer actuators. *Journal of Visualized Experiments*, 108:e53423, 2016.

[30] Luc Maffli, Samuel Rosset, Michele Ghilardi, Federico Carpi, and Herbert Shea. Ultrafast All-Polymer Electrically Tunable Silicone Lenses. *Advanced Functional Materials*, 25(11):1656–1665, 2015.

An open-loop control scheme to increase the speed and reduce the viscoelastic drift of dielectric elastomer actuators – Supplementary information

Alexandre Poulin[a], Samuel Rosset[b,*]

[a]*École polytechnique fédérale de Lausanne (EPFL), Soft Transducers Laboratory, Neuchâtel, Switzerland*
[b]*University of Auckland, Auckland Bioengineering Institute, Biomimetics Lab, Auckland, New Zealand*

Voltage-strain relation of an expending circle actuator

The in-plane expending circle actuator is one of the most common DEA configurations[1, 2]. It consists of a membrane with an equi-biaxial prestretch fixed to a circular frame, with a circular electrode at its centre. Despite this simple axi-symmetric geometry, calculating the strain of the active area as a function of the applied voltage is not trivial and requires solving a set of differential equations [3]. However, if the active area is much smaller than the membrane size, the expansion of the electrode leads to a negligible change of stretch state in the passive area of the actuator. The prestretch-induced force acting at the periphery of the active zone can therefore be assumed to be constant. Koh et al. have shown that there is negligible influence from the passive region of the membrane, if it is at least 5 times (preferably 10) larger than the active area [3]. Here, we therefore consider the case for which the membrane is much larger than the active area. The actuators used in this study have a 4 mm active area at the centre of a 44 mm membrane.

The equilibrium position of the actuator is defined when the sum of the elastic strain energy in the active zone, the prestretch-induced strain energy, and the electrostatic energy are minimised, and is therefore defined by:

$$\frac{\partial U_{el}}{\partial \lambda} - \frac{\partial U_{ps}}{\partial \lambda} - \frac{\partial U_{es}}{\partial \lambda} = 0, \tag{1}$$

where U_{el} is the elastic energy in the active area, U_{ps} is the prestretching energy, U_{es} is the electrostatic energy in the active area, and λ is the stretch ratio in the in-plane direction. For the equi-bixial expansion case considered here, the

---

*Corresponding author
Email addresses: `alexandre.poulin@epfl.ch` (Alexandre Poulin),
`s.rosset@auckland.ac.nz` (Samuel Rosset)

relation between the stretch ratio in the 3 principal directions can be obtained from the volume invariance: $\lambda_1 = \lambda_2 = \lambda$ and $\lambda_3 = \lambda^{-2}$.

We consider here an elastomer modelled with a Neo-Hookean strain energy density function:

$$w = \frac{\mu}{2}(I_1 - 3), \tag{2}$$

with μ the shear modulus of the material, and I_1 the first invariant of the stretch tensor: $I_1 = \lambda_1^2 + \lambda_2^2 + \lambda_3^2 = 2\lambda^2 + \lambda^{-4}$.

Therefore, the derivative of the elastic energy can be expressed as:

$$\frac{\partial U_{el}}{\partial \lambda} = V \frac{\partial w}{\partial \lambda} = V_0 \frac{\partial w}{\partial I_1} \frac{\partial I_1}{\partial \lambda} = A_0 t_0 \frac{\mu}{2} 4 \left(\lambda - \frac{1}{\lambda^5} \right) = 2 A_0 t_0 \mu \left(\lambda - \frac{1}{\lambda^5} \right), \tag{3}$$

where $V = V_0 = A_0 t_0$ are the volume of the active area, the initial volume of the active area (before prestretch and actuation), the initial surface of the active area, and the initial thickness of the membrane. We use the fact that elastomers keep a constant volume when deforming ($V = V_0 \lambda_1 \lambda_2 \lambda_3 = V_0$).

As mentioned above, we consider an active area much smaller than the membrane, and therefore, the derivative of the prestretch energy is independent of λ (i.e. constant force acting on the periphery of the active zone). To define it, we use the fact that in absence of an applied electric field, the system is in equilibrium. This situation corresponds to $U_{es} = 0$, and to $\lambda = \lambda_p$, where λ_p represents the equi-biaxial prestretch of the membrane. The equilibrium condition leads to:

$$\frac{\partial U_{ps}}{\partial \lambda} = \left. \frac{\partial U_{el}}{\partial \lambda} \right|_{\lambda = \lambda_p} = 2 A_0 t_0 \mu \left(\lambda_p - \frac{1}{\lambda_p^5} \right) \tag{4}$$

The electrostatic energy is the energy stored into the deformable capacitor C formed by the active area:

$$U_{es} = \frac{1}{2} C V^2 = \frac{\epsilon A_0 \lambda^2}{2 t_0 \lambda^{-2}} V^2 = \frac{\epsilon A_0 \lambda^4}{2 t_0} V^2, \tag{5}$$

where V is the applied voltage, and ϵ the permittivity of the elastomer. Partial derivation with respect to λ leads to:

$$\frac{\partial U_{es}}{\partial \lambda} = \frac{2 \epsilon A_0 \lambda^3}{t_0} V^2. \tag{6}$$

Finally, inserting Eqs. 3, 4, 6 into Eq. 1 leads to:

$$2 A_0 t_0 \mu \left(\lambda - \frac{1}{\lambda^5} - \lambda_p + \frac{1}{\lambda_p^5} \right) = \frac{2 \epsilon A_0 \lambda^3}{t_0} V^2 \tag{7}$$

$$V^2 = \frac{t_0^2 \mu}{\epsilon \lambda^3} \left(\lambda - \frac{1}{\lambda^5} - \lambda_p + \frac{1}{\lambda_p^5} \right), \tag{8}$$

which describes the relation between the applied voltage and the stretch ratio in the active zone of the membrane. The stretch ratio λ represents the total stretch

in the membrane, whereas in the case of DEAs, the important parameter is the actuation stretch λ_a, i.e. the expansion of the circular electrode. The actuation stretch is related to the total stretch of the membrane by the relation: $\lambda = \lambda_a \lambda_p$. Using this relation, we obtain the relation between the actuation stretch and the voltage:

$$V = \sqrt{\frac{t_0^2 \mu}{\epsilon(\lambda_a \lambda_p)^3} \left(\lambda_a \lambda_p - \frac{1}{(\lambda_a \lambda_p)^5} - \lambda_p + \frac{1}{\lambda_p^5} \right)}. \tag{9}$$

Finally, using the relation $\lambda_a = 1 + \varepsilon$ enables to establish a relation between the engineering actuation strain ε and the applied voltage.

Tuneable grating

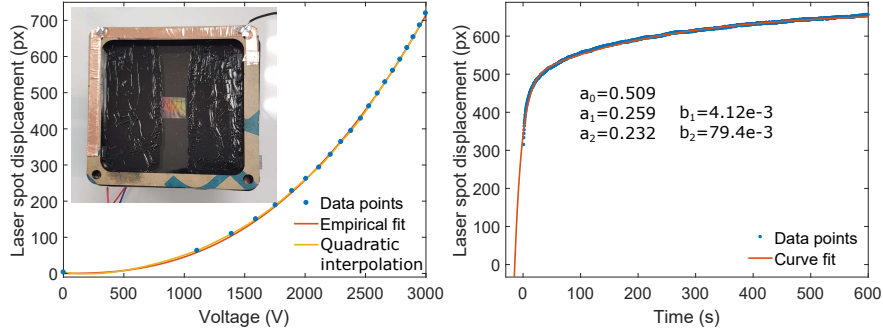

Figure S1: Left: Steady-state displacement of the first order difraction spot on the screen as a function of applied voltage and fit with the empirical KV^n model, as well as with quadratic Lagrangian interpolation. Inset: picture of the tuneable grating with electrodes on both sides of a soft silicone grating located at the centre. Right: spot displacement to a 3000 V voltage step input and fit with Eq. 8 and two time constants.

VHB at large strain

Figure 2b of the main article shows that the viscoelastic creep response of the VHB actuators is independent of strain for the tested strain range (up to 12.5 %). However, as VHB actuators can exhibit much larger strains, it is therefore useful to see what happens when they are driven at higher voltages. Figure S2 shows the strain of a VHB dot actuator for voltages steps of amplitude from 1700 V to 3000 V, leading to steady state strains from 5 % to 50 %. It can be seen that for strains up to 20 %, the response of the actuator is largely independent from the strain step amplitude, and the open-loop model can be applied. However, the figure shows a clear dependence of the viscoealstic creep parameters on the strain amplitude for strains higher than 20 %. In particular, the relative amplitude of the purely elastic response a_0 decreases from 0.5 for the lower voltage to 0.24 for the 3000 V step. Conversely, the relative amplitude

of the longer time constant increases, as shown by the slow continuous increase of the 3000 V step. A different model based on non-linear viscoelasticity should therefore be used for VHB actuators driven above 20 % strain. The actuator for this test was made on a membrane that was equi-biaxially prestretched by a factor of 3, and a different prestretch level may lead to a different behaviour.
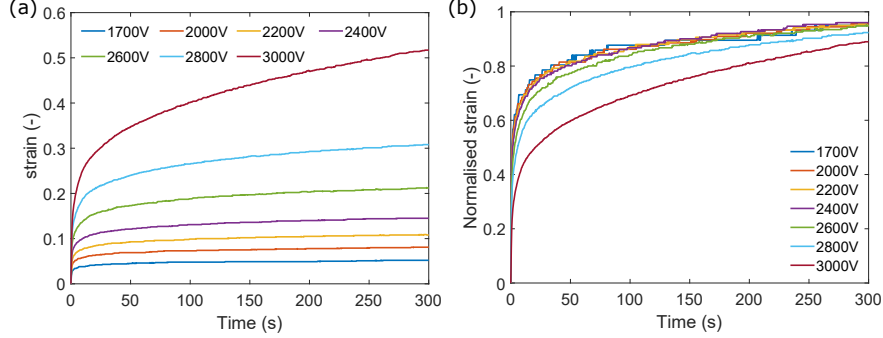

Figure S2: a) Voltage step test on a VHB dot actuator (equi-biaxial prestretch ratio of 3) for voltages from 1700 V to 3000 V. b) Normalised strain value.

References

[1] Federico Carpi, Iain Anderson, Siegfried Bauer, Gabriele Frediani, Giuseppe Gallone, Massimiliano Gei, Christian Graaf, Claire Jean-Mistral, William Kaal, Guggi Kofod, Matthias Kollosche, Roy Kornbluh, Benny Lassen, Marc Matysek, Silvain Michel, Stephan Nowak, Benjamin O'Brien, Qibing Pei, Ron Pelrine, Björn Rechenbach, Samuel Rosset, and Herbert Shea. Standards for dielectric elastomer transducers. *Smart Materials and Structures*, 24(10):105025, 2015.

[2] R. Pelrine, R. Kornbluh, Q. Pei, and J. Joseph. High-speed electrically actuated elastomers with strain greater than 100%. *Science*, 287(5454):836–839, 2000.

[3] S.J.A. Koh, T. Li, J. Zhou, X. Zhao, W. Hong, J. Zhu, and Z. Suo. Mechanisms of large actuation strain in dielectric elastomers. *Journal of Polymer Science, Part B: Polymer Physics*, 49(7):504–515, 2011.